MECHANICAL AND ELECTRICAL PROPERTIES OF ELECTRICALLY CONDUCTIVE NANOCOMPOSITES OF EPOXY/ POLYANILINE-COATED HALLOYSITE NANOTUBES

S. I. A. RAZAK[a,b*], I. I. MUHAMAD[a], N. F. A. SHARIF[b], N. H. M. NAYAN[b], A. R. RAHMAT[b], M. Y. YAHYA[c]

[a]*IJN-UTM Cardiovascular Engineering Centre, Universiti Teknologi Malaysia, 81310 Skudai, Johor, Malaysia.*
[b]*Polymer Engineering Department, Faculty of Chemical Engineering, Universiti Teknologi Malaysia, 81310 Skudai, Johor, Malaysia.*
[c]*Centre for Composites, Universiti Teknologi Malaysia, 81310 Skudai, Johor, Malaysia.*

This paper reports the preparation and characterization of newly developed conductive nanocomposites consisting of epoxy (EP) and polyaniline-coated halloysite nanotubes (HNT-PANI). The nanocomposites achieved its electrically conductive state (10^{-5} S·cm^{-1}) and improved impact strength (76 % increase compared to neat EP) with the addition of 12 wt% HNT-PANI. Such mechanically stable conductive nanocomposite could be useful in many applications such as electromagnetic interference shielding and charge dissipating material for secondary load bearing components plus the advantage of being cost effective.

1. Introduction

Halloysite nanotube (HNT) is a super-fine aluminosilicate, $Al_2Si_2O_5(OH)_4 \cdot 2H_2O$, with naturally occurring tubular structure at nanoscale [1]. Their tubular structures resemble that of carbon nanotubes in terms of aspect ratio and can be obtained at cheaper price. It has gained wide interest in the preparation of complex structures as an economically available nanotubular raw material. In addition, their similarity to layered clay like montmorillonite, make it possible to be intercalated/exfoliated chemically or physically. Recently, it has been utilized in electronic components [2], cosmetic products [3], pharmaceutics for drug-delivery [4], adsorbents [5], nanotemplates or nanoscale reaction vessels [6] and fillers in polymer nanocomposites [7].

Particularly in polymer nanocomposites, HNT can be regarded as suitable nanosized impact modifier to rigid polymer matrices such as epoxy (EP) [8-10]. Fracture toughness of EP was reported to be increased by 100 % by the addition of HNT [11]. On the other hand, electrically conductive EP composites have gained wide interest due to their promising properties for various applications such as electromagnetic shielding, sensors and electronic devices. The recent popular choice of conductive filler for EP is polyaniline (PANI) [12]. PANI is one of the most promising conducting polymers for industrial applications mainly due to its ease of preparation, excellent electrical, optical, and magnetic properties [13-15]. The main disadvantage of this type of composite is that the mechanical properties deteriorate with the inclusion of PANI [16]. For that reason it is interesting to combine the reinforcement capability of HNT and the conductance of PANI because the demands for materials having a combination of a wide range of desirable properties are always increasing.

---

[*]Corresponding author: saifulizwan@utm.my

A feasible approach to design such a material is by modifying or coating the HNT by PANI. Many works have been done to form PANI coating on HNT in order to improve physical, mechanical, and electrical properties [17-20]. The most common method of doping the HNT-PANI is by using mineral acid. The drawbacks of it are that the dopant might destroy the crystal structure of the HNT and renders limited solubility in common solvents and polymer matrices [21]. Our earlier work reported a simple modification by using a bifuctional dopant to introduce charge instability to the HNT-PANI without destroying the nanoclays [22].

Therefore in order to achieve a conductive nanocomposite with good mechanical properties, we suggest a simple method to utilize our earlier developed HNT-PANI nano-filler incorporated in EP. It is expected that the HNT-PANI could induce electron conduction and better surface interactions without destroying the EP matrix mechanical integrity. Thus the main aim of this study is to prepare conductive nanocomposites of EP/HNT-PANI with stable and improved mechanical properties.

2. Experimental

2.1 Preparation of EP/HNT-PANI Nanocomposites

The PANI-coated HNT (HNT-PANI) were prepared by the in situ chemical oxidative polymerization technique. Detail description of the preparation method was described earlier elsewhere [22]. Briefly, the monomer, dopant and oxidant used were aniline (Acros), para-hydroxybenzenesulfonic acid (Sigma) and ammonium persulfate (Merck), respectively. The prepared HNT-PANI were dispersed in EP resin, diglycidyl ether of bisphenol-A (DGEBA, Sigma) at 70°C under stirring for 60 min and then degassed. The hardener, trifluoroboron (4-chlorobenzeneamine) (Air Products, USA), was added (10 phr to EP) and mixed at room temperature. The precured nanocomposites were then degassed for 30 min and cast into silicon rubber molds of the required dimensions and left for cure at room temperature. Following this procedure, EP/HNT-PANI nanocomposites with the required HNT-PANI loading were prepared. Neat PANI was prepared for comparison purposes.

2.2 Characterizations

The tensile test (ASTM D638) was performed using a computer controlled Instron machine, with a crosshead speed of 5 mm/min, at a standard laboratory atmosphere of 23°C. The flexural test (ASTM D790) was performed by three point bending configuration at 3 mm/min, under ambient conditions. Izod impact strength was measured on un-notched specimens according to the ASTM D256, using a pendulum type impact tester. At least five replicates for each sample were tested. The DC conductivity was measured on samples of circular dimension, using a resistance meter (Advantest) by the four-probe method, under ambient conditions. Samples were stored in a desiccator filled with silica gels, prior to testing, to remove adsorbed moisture. Five measurements were made on each sample. UV-visible spectra of the EP composites were obtained using a Shimadzu UV-vis spectrophotometer, with the samples suspended in dimethylsulfoxide. Fourier transform infrared (FTIR) spectra of the samples were obtained using a model 2000 Perkin Elmer spectrometer with a resolution of 0.4 cm^{-1}. The tensile fractured surface morphology of the nanocomposites was analyzed using a scanning electron microscope (SEM), Leo Supra 50VP.

3. Results and discussion

3.1 Mechanical Properties

Mechanical properties of the nanocomposites can be summarized in Table 1. Tensile strength of the EP loaded with 1 wt% unmodified HNT shows slight improvement compared to that of neat cured EP.

Table 1: Mechanical properties of EP and its EP/HNT-PANI nanocomposites.

Sample	Tensile		Flexural		Impact Strength (KJ/m^2)
	Strength (MPa)	Modulus (GPa)	Strength (MPa)	Modulus (GPa)	
EP	74.1 ± 0.7	2.68 ± 0.13	155.7 ± 3.3	3.86 ± 0.05	10.54 ± 0.48
EP/1HNT	76.3 ± 1.2	2.69 ± 0.82	157.5 ± 1.8	3.89 ± 0.04	13.53 ± 0.33
EP/1HNT-PANI	76.8 ± 1.1	2.27 ± 0.37	157.8 ± 4.6	3.88 ± 0.07	15.75 ± 0.74
EP/5HNT-PANI	76.2 ± 1.8	2.42 ±0.08	158.3 ± 2.7	3.92 ± 0.06	16.61 ± 1.20
EP/9HNT-PANI	75.7 ± 0.8	2.54 ± 0.12	157.4 ± 9.2	3.91 ± 0.15	17.32 ± 0.88
EP/12HNT-PANI	68.2 ± 0.3	2.33 ±0.46	152.4 ± 1.1	3.84 ± 0.08	18.60 ± 0.53
EP/15HNT-PANI	41.7 ± 2.4	1.28 ± 0.43	140.6 ± 1.3	3.14 ± 0.12	11.84 ± 0.25

Its PANI modified HNT counterpart induces similar positive changes to the EP. Similar values were recorded for higher amount of HNT-PANI up to 9 wt%. This is an encouraging indication that the presence of PANI on the HNT does not lower the tensile strength of EP. However, EP/12HNT-PANI sample reveals a slight reduction compared to neat EP. This can be associated with the nanoclay agglomeration, which lead to contact percolation between bound PANI of one HNT with another. This percolation might lead to less interfacial bonding between EP and HNT-PANI. Further inclusion of the 15 wt% PANI modified HNT into the EP revealed a major drop in the tensile strength. This can be caused by the poor curing reaction of the resin and the hardener. Tensile modulus of the EP exhibit no marked changes with the incorporation of unmodified HNT nor increasing HNT-PANI up to 12 wt.%. The deterioration at 15 wt% HNT-PANI is mainly because of three reasons (1) reduced crosslinking network of the EP matrix due to the high HNT-PANI agglomeration, (2) inherent brittle nature of PANI and (3) difference in polarity and crystallinity of the two polymers (PANI and EP). Thus no efficient load transfer occurred from the EP to the HNT-PANI component at this particular loading. Flexural strength is a measure of the ability of the material to withstand bending forces applied perpendicular to its longitudinal axis.

In flexural testing, multiple mechanisms such as tension, shearing, and compression take place simultaneously. Both flexural strength and modulus of the EP loaded unmodified HNT show slight increment compared to that of neat EP. The improvement was maintained with the inclusion of HNT-PANI. The flexural properties of the nanocomposites seems to be unaffected by the discrete HNT-PANI and the intermediate conducting networks. By contrast, noticeable reductions are observed at 15 wt% loading, owing to the highly agglomerated HNT-PANI. Impact strength is defined as the ability of a material to resist fracture under stress applied at high speed.

The impact properties of composite materials are directly related to overall toughness. EP resins are inherently brittle and rigid, with low impact strength and poor resistance to crack propagation. The uncoated HNT nanocomposites show greater impact resistance compared to that of neat EP, as they interact with the crack formation in the matrix and act as a stress transferring medium. Adding merely 1 wt% HNT increased the impact strength of EP by 28 %. Comparatively, the nanocomposite with 1 wt% HNT-PANI induces even more impact resistance to its uncoated HNT counterpart. The presence of PANI on the surface of HNT promotes greater impact to the EP composite, attributable to the PANI-EP interaction that imparts matrix interface molecular chain flexibility, resulting in additional energy absorbing capacity. This observation can be explained by the high surface area of the nano-sized and non-percolated HNT-PANI that produces new frictional work, resulting from the displacement between the EP matrix and HNT-PANI, which increases the impact resistance of the nanocomposites by slowing crack growth during fracture.

However, the EP/15HNT-PANInanocomposite reveals no further improvement, which might be caused by the brittleness promoted by the high percolating HNT-PANI networks.

3.2 DC Conductivity

Table 2 shows the DC conductivity of the EP and its nanocomposites. Inclusion of 1 wt% of HNT to the EP revealed no changes to the matrix electrical conductance. Moreover inclusion of HNT-PANI up to 5 wt% shows no changes and also being accompanied by the 10^1 magnitude increase for the EP/9HNT-PANI sample. This shows that the nanocomposites are still in their insulating state. The fillers could not induce any significant DC conductivity because no continuous conducting network is formed, thus the bulk is dominated by the insulating EP matrix. Meanwhile the conductivity at 12 wt% loading jumps drastically to 10^{-5} S·cm^{-1}. This is an indication that the electrical percolation threshold of the HNT-PANI has been reached. When percolation concentration is reached, the conductivity increased dramatically because the HNT-PANI has created joint 3D conductive pathways throughout the EP matrix. The network is illustrated in Figure 1. A conductive composite with low percolation threshold is preferred because low percolation lowers the cost and minimizes influences on the mechanical properties.

Table 2: DC conductivity of EP and its EP/HNT-PANI nanocomposites.

Sample	DC Conductivity, σ (S·cm^{-1})
EP	10^{-13}
EP/1HNT	10^{-13}
EP/1HNT-PANI	10^{-13}
EP/5HNT-PANI	10^{-13}
EP/9HNT-PANI	10^{-12}
EP/12HNT-PANI	10^{-5}
EP/15HNT-PANI	10^{-5}
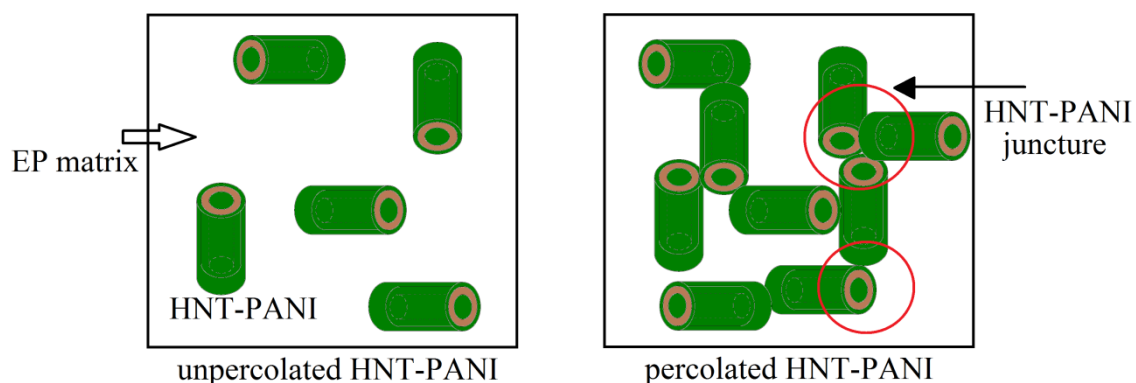
Fig. 1: Unpercolated and percolated state of HNT in EP matrix.

3.3 UV-visible Spectroscopy

Fig. 2 presents the UV-visible spectra of the samples. The UV-visible spectrum of EP/1HNT (Figure 2a) shows no obvious absorption spectra across the spectrum, indicating that no spectral transition occurs along the measured wavelength. This corroborates its electrically insulating state. The neat prepared PANI (Figure 2b) presents the π-π* (279 nm) and the polaron-π* (442 nm) which corresponds to the electron orbital transitions along the backbone of conducting PANI chains [25]. Meanwhile, the small peak at around 660 nm can be assigned to the

isolated polaron band. The broad peak at around 900 nm represents the combination of π-polaron transitions, which resulted in "free carrier tail". The EP/1HNT-PANI sample (Figure 2c) reveals the existence of PANI isolated polaron band transitions, but with much lower intensity, prohibited by the EP matrix and the HNT. Furthermore, no delocalized polaron peak is observed. It can be said that HNT-PANI component keeps the doped condition inside the EP matrix, but is insufficient to promote any carrier mobility. Band diagrams of the transitions are depicted in the insert of Figure 2. It can be observed that the addition of 12 wt% HNT-PANI induces the existence of conjugation peaks (279 and 442 nm). The 900 nm peak appears to be present in the sample which is related to the lower energy polaronic transition of the dispersed HNT-PANI. The transition peak appears to be broader than the neat PANI, due to the combination of PANI networks along the HNT surface and throughout the EP matrix. The observed depletion of the 660 nm peak indicates that the isolated polaron has interacted with its adjacent unit, therefore creating a broader polaron absorbance peak (900 nm) with more dispersed energy, which is more delocalized.
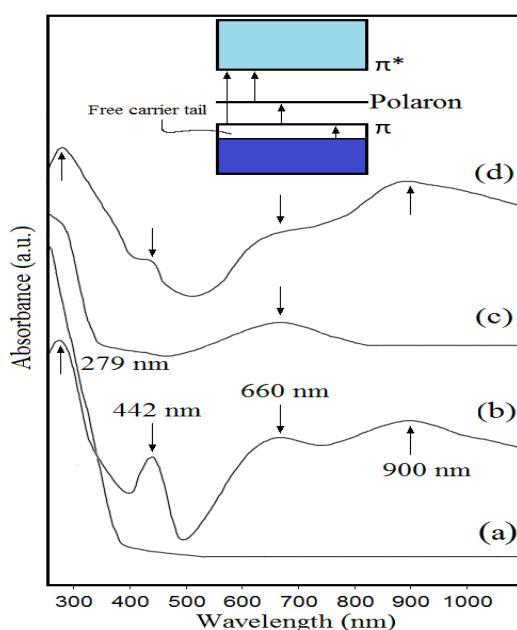
Fig. 2: UV-visible spectra of a) EP/1HNT, b) neat PANI, c) EP/1HNT-PANI, (d) EP/12HNT-PANI.

3.4 FTIR Spectroscopy

Fig. 3 depicts the FTIR spectra of the samples. The FTIR spectrum of EP/1HNT (Figure 3a) shows the characteristic of cured bisphenol-A epoxy, no significant vibrational peaks originating from the HNT component can be observed. The spectrum of neat PANI (Figure3b) exhibits the presence of benzoid and quinoid ring vibration at 1530 cm^{-1} and 1575 cm^{-1}, respectively, indicating the oxidation state of the conducting emeraldine salt of PANI. The strong peak at 1140 cm^{-1} is the characteristic peak of PANI conductivity and is a measure of the degree of delocalization of electrons. The weak and small peak at 3230 cm^{-1} is assigned to the N-H stretching mode. Spectrum of the conductive nanocomposite sample (EP/12HNT-PANI) presents several new peaks associated with the adhered PANI. However, the sample shows no significance detection of HNT-related vibrational bands (Si-O-Si and Si-O). This signifies that the nanotubes have been occupied by PANI [22]. The essential point to be noted is that the existence of 1140 cm^{-1} peak, which indicates that the bound PANI component still keeps the doped conducting condition in the EP matrix. This condition is vital for ensuring that the incorporated HNT-PANI nano-particles do not deprotonate. The intense quinoid ring vibration suggests that the presence of HNT promotes a more stable PANI quinoid ring structure. The slight emergence of N-H stretching implies that charge-transfer activity between the conducting PANI chains (bound and junction) can occur. These vibrations ultimately indicate that a conductive composite has been achieved. The interaction between N-H of PANI and the dopant ion (protonation) is responsible for the

enhancement, whereby the dopant ion can disturb the H-bond, resulting in an increase in N-H stretching intensity. Furthermore, this interaction is responsible for the charge transfer and polaron creation which resulted in the increase in the degree of conductivity. Interactions between the components are shown in Figure 4.
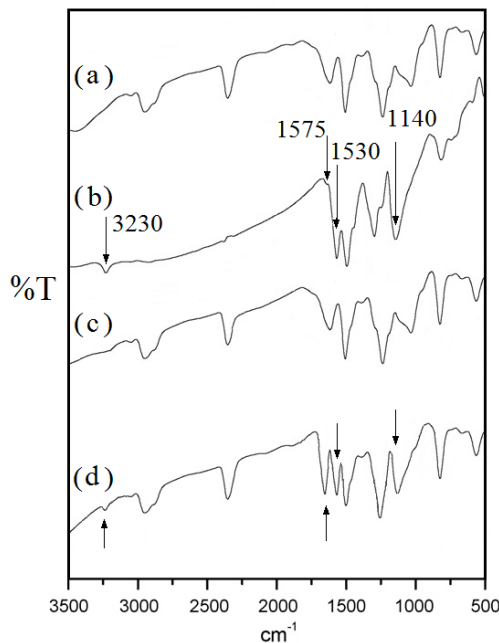
Fig. 3: FTIR spectra of a) EP/1HNT, b) neat PANI, c) EP/1HNT-PANI, d) EP/12HNT-PANI.
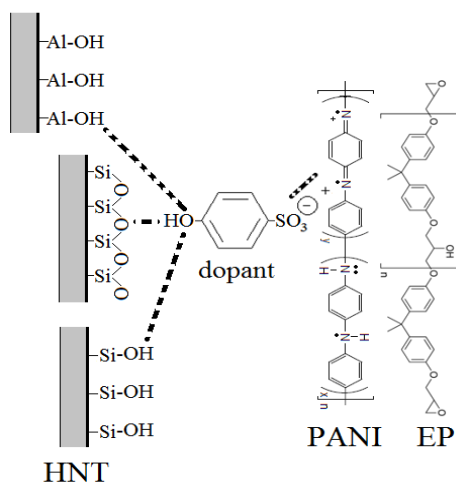
Fig. 4: Surface interactions of the nanocomposite.

3.5 Fracture Morphology

SEM image of the modified HNT is given in Figure 5a. It can be seen that the surface had been deposited by PANI without destroying the clays tubular structure. Tensile fractured surface of the conductive nanocomposite (EP/12HNT-PANI) are shown in Figure 5b and c. The fractured surface (Figure 5b) reveals distinct continuous HNT-PANI particles within the EP matrix. A higher magnification (Figure 5c) indicates presence of the nanotubes. Though the conductive fillers were at its network state, they are able to provide reinforcement towards the matrix. It can be believed that the HNT-PANI failed by pull-out of individual tubes rather than its percolated bundle. Furthermore the exposed matrix relates to good matrix-modified HNT adhesion. Depiction of the pull-out of the percolated HNT-PANI is given in Figure6.
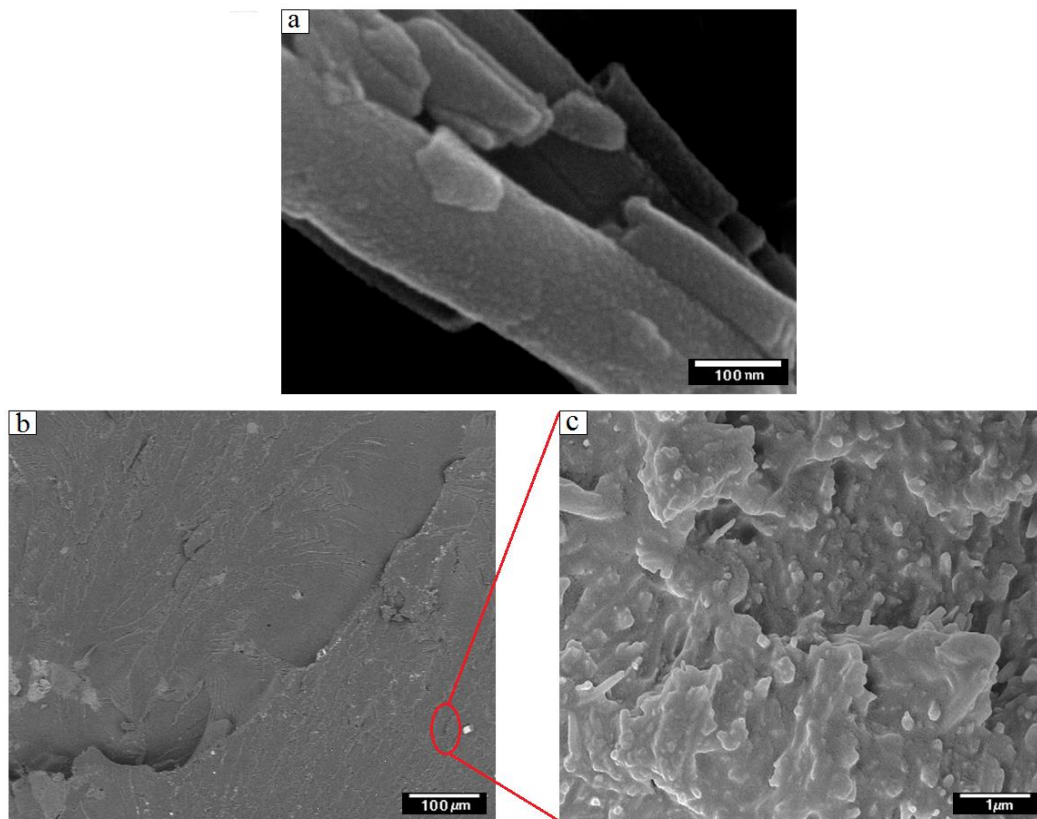
Fig. 5: SEM a) micrograph of HNT-PANI, b-c) fractured surface of EP/12HNT-PANI.
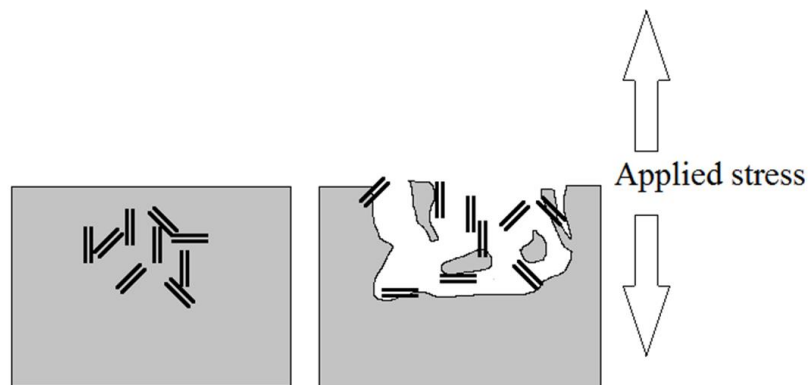
Fig. 6: Depiction of pull-out of HNT-PANI from the EP matrix.

4. Conclusions

It can be concluded that the EP/12HNT-PANI nanocomposite sample seemed to be the most desirable formulation based on the conductivity transformation and improvement in mechanical properties, particularly the impact strength. The nanocomposite showed transformation from insulating to conductive state with the inclusion of the modified nanoclay. The FTIR and UV-visible revealed desirable vibrational and transition peaks which correspond to the nanocomposites electronic properties. In term of its mechanical properties, the PANI-HNT was effective in increasing the impact strength of the EP without sacrificing other vital properties such as tensile and flexural. The morphology revealed favourable failure characteristic that justify the nanocomposites mechanical stability. This newly improved material can be ideal for applications which require mechanical integrity, slow crack growth plus being electrically conductive. Though

maybe not be suitable to be used for primary load bearing parts, this nanocomposite might be useful for secondary structures such as electromagnetic interference shielding material in aircraft structures or charge dissipating material in electrical components.

Acknowledgement

References

[1] D. Rawtani, Y. K. Agrawal, Reviews on Advanced Materials Science, **30**, 282 (2012).
[2] D. Fix, D. V. Andreeva, Y. M. Lvov, D. G. Shchukin, H. Möhwald, Advanced Functional Materials, **19**,1720 (2009).
[3] Y. M. Lvov, D. G. Shchukin, H. Mohwald, R. R. Price, ACS Nano, **2**, 814 (2008).
[4] C. Aguzzi, P. Cerezo, C. Viseras, C. Caramella, Applied Clay Science, **36**, 22 (2007).
[5] P. Luo, Y. Zhao, B. Zhang, J. Liu, Y. Yang, J. Liu, Water Research, **44**,1489 (2010).
[6] Y. Liu, Q. Cai, H. Li, J. Zhang, Journal of Applied Polymer Science, **128**, 517 (2013).
[7] N. F. A. Sharif, Z. Mohamad, A. Hassan, M. U. Wahit, Journal of Polymer Research, **19**, 1 (2012).
[8] S. Deng, J. Zhang, L. Ye, Composites Science and Technology, **69**, 2497 (2009).
[9] V. Vahedi, P. Pasbakhsh, Polymer Testing, **39**, 101 (2014).
[10] M. Liu, B. Guo, M. Du, Y. Lei, D. Jia, Journal of Polymer Research, **15**, 205 (2008).
[11] Y. Tang, S. Deng, L. Ye, C. Yang, Q. Yuan, J. Zhang, C. Zhao, Composites Part A, **42**, 345 (2011).
[12] Z. Qiang, G. Liang, A. Gu, L. Yuan, Journal of Nanoparticle Research, **16**, 1 (2014).
[13] D. H. Cho, H. Yashiro, Y. K. Sun, S. T. Myung, Journal of The Electrochemical Society, **161**, A142 (2014).
[14] I. Ozaytekin, Polymer Composites, **35**, 372 (2014).
[15] W. E. Mahmoud, Y. C. Chang, A. A. Al-Ghamdi, F. Al-Marzouki, L. M. Bronstein, Polymer Composites, **34**, 299 (2013).
[16] S. I. A. Razak, W. A. W. A. Rahman, M. Y. Yahya, NANO, **7**, 1250039 (2012).
[17] C. Zhou, X. Du, Z. Liu, Y. W. Mai, S. P. Ringer, Journal of Materials Science, **46,** 446 (2011).
[18] W. L. Zhang, H. J. Choi, Colloid and Polymer Science, **290**, 1743 (2012).
[19] L. Zhang, T. Wang, P. Liu, Applied Surface Science, **255**, 2091 (2008).
[20] X. Sun, Y. Long, P. Wang, J. Sun, J. Ma, Reactive and Functional Polymers, **72**, 323 (2012).
[21] A. Rahy, T. Rguig, S. J. Cho, C. E. Bunker, D. J. Yang, Synthetic Metals, **161**, 280 (2011).
[22] S. I. A. Razak, N. F. A. Sharif, I. I. Muhamad, Composite Interfaces, **21**, 715 (2014).
[23] S. I. A Razak, A. L Ahmad, S. H. S. Zein, A. R. Boccaccini, Scripta Materialia, **61**, 592 (2009).